MULTIPHYSICS MODELING VOLUME 6

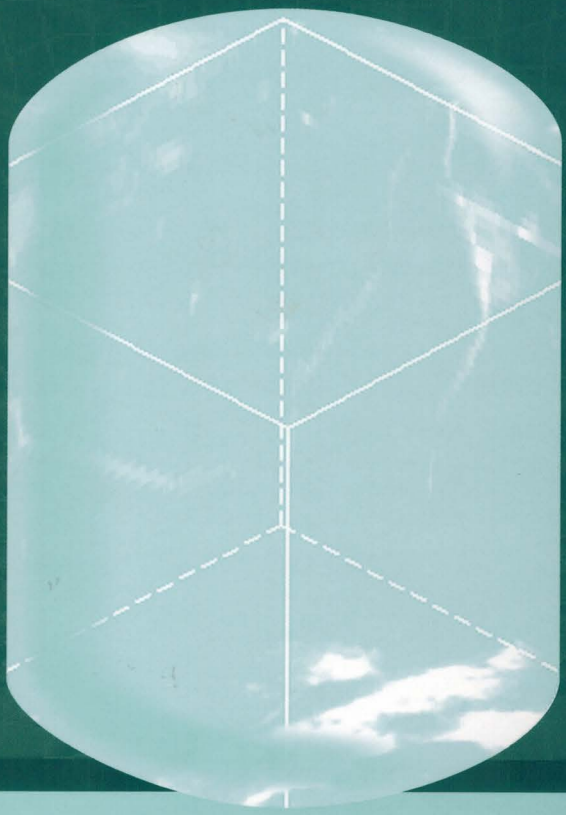

$$\mathbf{u} = -\frac{\mathbf{k}}{\mu} \cdot (\nabla p - \rho g \nabla z)$$

Mathematical and Numerical Modeling in Porous Media: Applications in Geosciences

Martín A. Díaz Viera, Pratap N. Sahay, Manuel Coronado and Arturo Ortiz Tapia
EDITORS

CRC Press
Taylor & Francis Group
A BALKEMA BOOK

Mathematical and Numerical Modeling in Porous Media: Applications in Geosciences

Editors

Martín A. Díaz Viera

Instituto Mexicano del Petróleo (IMP), México

Pratap N. Sahay

Centro de Investigación Científica y de Educación Superior de Ensenada (CICESE), México

Manuel Coronado

Instituto Mexicano del Petróleo (IMP), México

Arturo Ortiz Tapia

Instituto Mexicano del Petróleo (IMP), México

CRC Press
Taylor & Francis Group
Boca Raton London New York Leiden

CRC Press is an imprint of the
Taylor & Francis Group, an **informa** business

A BALKEMA BOOK

CRC Press/Balkema is an imprint of the Taylor & Francis Group, an informa business

Typeset by MPS Limited, Chennai, India
Printing and binding by PrintSupport4U, Meppel, The Netherlands

Published by: CRC Press/Balkema
P.O. Box 447, 2300 AK Leiden, The Netherlands
e-mail: Pub.NL@taylorandfrancis.com
www.crcpress.com – www.taylorandfrancis.com

Library of Congress Cataloging-in-Publication Data

Mathematical and numerical modeling in porous media : applications in geosciences / Martín A. Diaz Viera . . . [et al.].
p. cm. – (Multiphysics modeling, ISSN 1877-0274 ; v. 6)
Includes bibliographical references and index.
ISBN 978-0-415-66537-7 (hardback) – ISBN 978-0-203-11388-2 (ebook)
1. Geophysics–Mathematical models. 2. Porous materials–Mathematical models.
I. Diaz Viera, Martín A.
QC809.M37M38 2012
550.1′51–dc23

2012000068

ISBN: 978-0-415-66537-7 (Hbk)
ISBN: 978-0-203-11388-2 (eBook)

Section 3: Statistical and stochastic characterization

CHAPTER 11

Joint porosity-permeability stochastic simulation by non-parametric copulas

V. Hernández-Maldonado, M. A. Díaz-Viera & A. Erdely-Ruiz

11.1 INTRODUCTION

On geological-petrophysical reservoir modeling exists the need to establish dependence models between petrophysical properties, such as porosity-permeability relationship. In practice, there is little information about permeability while the porosity is mostly sampled. By modeling the dependence structure between this two properties, it is possible to know the permeability profile through the available information on the porosity one.

In order to calculate permeability profiles in wells, typically is used a linear estimator in a regression form, see Balam (1995). However, to predict the average, or expected value of a property exists the disadvantage of not reproducing the the variability of the data and consequently, the estimated profiles do not reproduce the extreme values of the real information. This situation is critical when a reservoir is been modeled because this values may represent impermeable barriers or high permeability zones.

A competitive and much more systematic method was proposed by Deutsch & Cockerham (1994). It uses the application of multivariate stochastic simulations in order to predict the permeability or primary variable; where a proper specification of the petrophysical properties dependence structure is crucial. This approach involves the application of simulated annealing technique to model the joint distribution function of the porosity-permeability relation.

A modification of Deutsch's methodology was proposed by Díaz-Viera and Casar-González (2005). In that work, it was proposed the use of a bivariate t-copula to construct the joint distribution function rather than use the sampling one, also the dependence structure is specified by matching measures such as Kendall's τ and Spearman ρ. The above methodology was applied to simulate the permeability from the porosity profile in a double porosity carbonate systems restricted to one-dimensional case at well-log scale Díaz-Viera et al. (2006).

While Díaz-Casar methodology can reproduce adequately the observed data, and also their extreme values using the t-copula, the critical problem of this proposal is that the copula used is parametric type, i.e. it is based on a given distribution function, the student t. This causes the data not to be naturally represented, because the real data distribution is hard to fit properly with only one parametric distribution.

The methodology presented here makes co-dependent geostatistical simulations using Bernstein copulas, which have the ability to model the dependence structure between random variables, as petrophysical properties, without assume a given distribution function as t-copulas do.

11.2 NON-CONDITIONAL STOCHASTIC SIMULATION METHODOLOGY BY USING BERNSTEIN COPULAS

The proposed method is based on Díaz-Viera's modification to Deutsch and Cockerham methodology for geostatistical simulation. Broadly speaking the methodology can be described in two stages. The first one is to carry out a non-parametric permeability (K) simulation by Bernstein copulas, using the porosity (PHI) as secondary variable. At this stage we are reproducing the joint dependence pattern between these two petrophysical properties. In the second one, a geostatistical

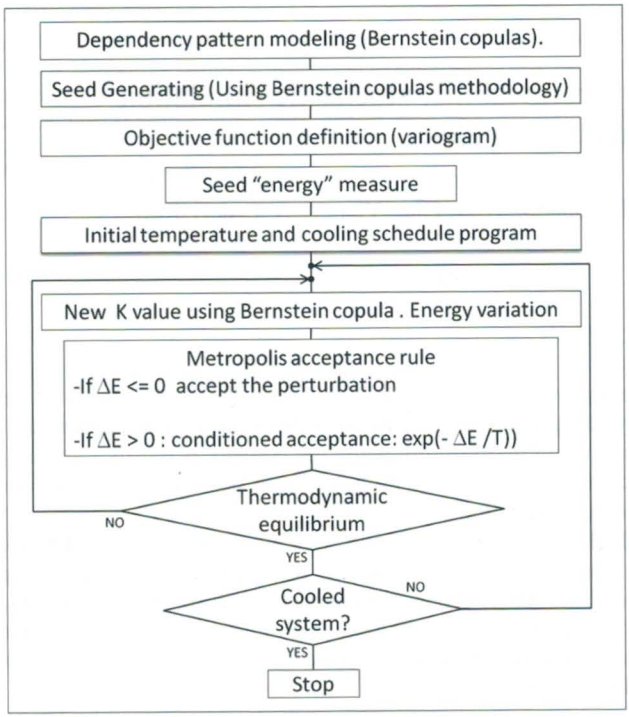

Figure 11.1 Methodology diagram. It shows the steps to produce a geostatistical co-simulation by simulated annealing, using Bernstein copulas.

simulation of permeability is performed by simulated annealing method, whose objective function is the variogram model, see Deutsch & Journel (1998), Figure 11.1.

A more detailed description of each step of the methodology is described below:

1. Modeling the petrophysical properties dependence pattern, using non-parametric copulas or Bernstein copulas.
2. Generating the seed or initial configuration for simulated annealing method, using the non-parametric simulation algorithm.
3. Defining the objective function.
4. Measuring the energy of the seed, according to the objective function.
5. Calculating the initial temperature and the simulated annealing schedule using the methodology proposed by Dreo et al. (2006).
6. Performing the simulation:
   - Accept or reject a new proposed permeability value using the non-parametric simulation algorithm.
   - The simulation finalizes when the objective function error (previously defined) is reached; an accumulation of 3 stages without change occurs; or when the maximum attempted perturbations is reached.

11.3 APPLICATION OF THE METHODOLOGY TO PERFORM A NON-CONDITIONAL SIMULATION WITH SIMULATED ANNEALING USING BIVARIATE BERNSTEIN COPULAS

We propose a copula-based non-parametric approach to model the relationship between the permeability and porosity of the double porosity carbonate formations of a South Florida Aquifer

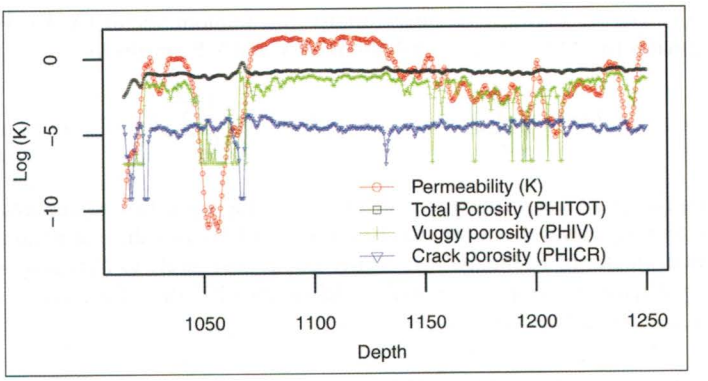

Figure 11.2 Crack porosity (PHICR), vuggy porosity (PHIV), total porosity (PHITOT) and permeability (K) derived from NMR Log (K).

in the western Hillsboro Basin of Palm Beach County, Florida, see Figure 11.2. After that, this methodology models the spatial distribution of the permeability in function of the depth.

The characterization of this aquifer for the borehole and field scales is given in Parra et al. (2001) and Parra & Hackert (2002), and a hydrogeological situation is described by Bennett et al. (2002). The interpretation of the borehole data and determination of the matrix and secondary porosity and secondary-pore types (shapes of spheroids approximating secondary pores) were presented by Kazatchenko et al. (2006a), where to determine the pore microstructure of aquifer carbonate formations the authors applied the petrophysical inversion technique that consists in minimizing a cost function that includes the sum of weighted square differences between the experimentally measured and theoretically calculated logs as in Kazatchenko et al. (2004).

In this paper we used the results of inversion obtained by Kazatchenko et al. (2006a) for carbonate formations of South Florida Aquifer that includes the following petrophysical characteristics: matrix porosity, secondary vuggy and crack porosities. It should be noted that the secondary-porosity system of this formation has complex microstructure and corresponds to a model with two types of pore shapes: cracks (flattered ellipsoids) with the overall porosity of 2% and vugs (close to sphere) with the porosity variations in the range of 10–30%. Such a secondary-porosity model can be interpreted as the interconnected by microfractures and channels vuggy formation.

The details of the statistical properties analysis of the sampled data were largely explained by Díaz-Viera et al. (2006), based on this study we determine that the highest observed dependence between the petrophysical properties corresponds to vuggy porosity (PHIV) and permeability (K).

11.3.1 *Modeling the petrophysical properties dependence pattern, using non-parametric copulas or Bernstein copulas*

According to Sklar's Theorem, see Sklar (1959), the underlying bivariate copula associated to a bivariate random vector (X, Y) represents a functional link between the joint probability distribution H and the univariate marginal distributions F and G, respectively:

$$H(x, y) = C(F(x), G(y)) \tag{11.1}$$

for all x, y in the extended real numbers system, where $C : [0, 1]^2 \to [0, 1]$ is unique whenever X and Y are continuous random variables. Therefore, all the information about the dependence between random variables is contained in their corresponding copula. Several properties may be derived for copulas, see Schweizer & Sklar (1983) and Nelsen (2006), and among them we have an immediate corollary from Sklar's Theorem: X and Y are independent continuous random variables if and only if their underlying copula is $\Pi(u, v) = uv$.

Let $\mathcal{S} := \{(x_1, y_1), \ldots, (x_n, y_n)\}$ be observations of a random vector (X, Y). We may obtain empirical estimates for the marginal distributions of X and Y by means of

$$F_n(x) = \frac{1}{n}\sum_{k=1}^{n} \mathbb{I}\{x_k \leq x\}, \qquad G_n(y) = \frac{1}{n}\sum_{k=1}^{n} \mathbb{I}\{y_k \leq y\}, \tag{11.2}$$

where $\mathbb{I}$ stands for an indicator function which takes a value equal to 1 whenever its argument is true, and 0 otherwise. It is well-known, see Billingsley (1995), that the empirical distribution F_n is a consistent estimator of F, that is, $F_n(t)$ converges almost surely to $F(t)$ as $n \to \infty$, for all t.

Similarly, we have the empirical copula, Deheuvels (1979), a function C_n with domain $\{i/n : i = 0, 1, \ldots, n\}^2$ defined as

$$C_n\left(\frac{i}{n}, \frac{j}{n}\right) = \frac{1}{n}\sum_{k=1}^{n} \mathbb{I}\{rank(x_k) \leq i, rank(y_k) \leq j\} \tag{11.3}$$

and its convergence to the true copula C has also been proved, see Fermanian et al. (2004). The empirical copula is not a copula, since it is only defined on a finite grid, not in the whole unit square $[0, 1]^2$, but by Sklar's Theorem, see Sklar (1959), C_n may be extended to a copula.

We model vuggy porosities as an absolutely continuous random variable X with unknown marginal distribution function F, and permeability as an absolutely continuous random variable Y with unknown marginal distribution function G. We have bivariate observations from the random vector (X, Y). For simulation of continuous random variables, the use of the empirical distribution function estimates Eq. (11.2) is not appropriate since F_n is a step function, and therefore discontinuous, so a smoothing technique is needed. Since our main goal is simulation of porosity-permeability, it will be better to have a smooth estimation of the marginal quantile function $Q(u) = F^{-1}(u) = \inf\{x : F(x) \geq u\}$, $0 \leq u \leq 1$, which is possible by means of Bernstein polynomials as in Muñoz-Pérez & Fernández-Palacín (1987).

$$\tilde{Q}_n(u) = \sum_{k=1}^{n} \frac{1}{2}(x_k + x_{k+1})\binom{n}{k} u^k (1-u)^{n-k} \tag{11.4}$$

and the analogous case for marginal G in terms of values y_k. For a smooth estimation of the underlying copula we make use of the Bernstein copula as in Sancetta & Satchell (2004) and Sancetta (2007):

$$\tilde{C}_n(u, v) = \sum_{i=1}^{n}\sum_{j=1}^{n} C_n\left(\frac{i}{n}, \frac{j}{n}\right)\binom{n}{i} u^i (1-u)^{n-i}\binom{n}{j} v^j (1-v)^{n-j} \tag{11.5}$$

for every (u, v) in the unit square $[0, 1]^2$, and where C_n is as defined in Eq. (11.3).

11.3.2 *Generating the seed or initial configuration for simulated annealing method, using the non-parametric simulation algorithm*

In order to simulate replications from the random vector (X, Y) with the dependence structure inferred from the observed data $\mathcal{S} := \{(x_1, y_1), \ldots, (x_n, y_n)\}$, accordingly to a result in Nelsen (2006), we have the following algorithm:

1. Generate two independent and continuous uniform $(0, 1)$ random variates u and t
2. Set $v = C_u^{-1}(t)$ where

$$C_u(v) = \frac{\partial \tilde{C}(u, v)}{\partial u} \tag{11.6}$$

and $\tilde{C}$ is obtained by (Eq. 11.5)

3. The desired pair is $(x, y) = (\tilde{Q}_n(u), \tilde{R}_n(v))$, where $\tilde{Q}_n(u)$ and $\tilde{R}_n(v)$, are the estimated and smoothed quantile functions of X and Y, respectively, according to (Eq. 11.4).

This non-parametric simulation methodology is used to generate the initial configuration or seed, which is used as a start point in the metropolis algorithm. The Figure 11.3 shows the resulting non-conditional simulation, note that the Bernstein copula reproduces very well the marginal distribution of each petrophysical property and do the same with the joint distribution function, therefore, the complex dependence structure existing between this two properties, vuggy porosity (PHIV) and permeability (K), is very well described by the non-parametric copulas.

Also note that the copula can reproduce the variability and the extreme values of the original data. This is verified, comparing some of most relevant statistics of the real and simulated permeability values using the Bernstein copulas, Figure 11.4.

Finally, Figure 11.5 shows the spatial distribution of permeability vs. a simple non-conditional Bernstein copulas simulation, using PHIV as secondary variable.

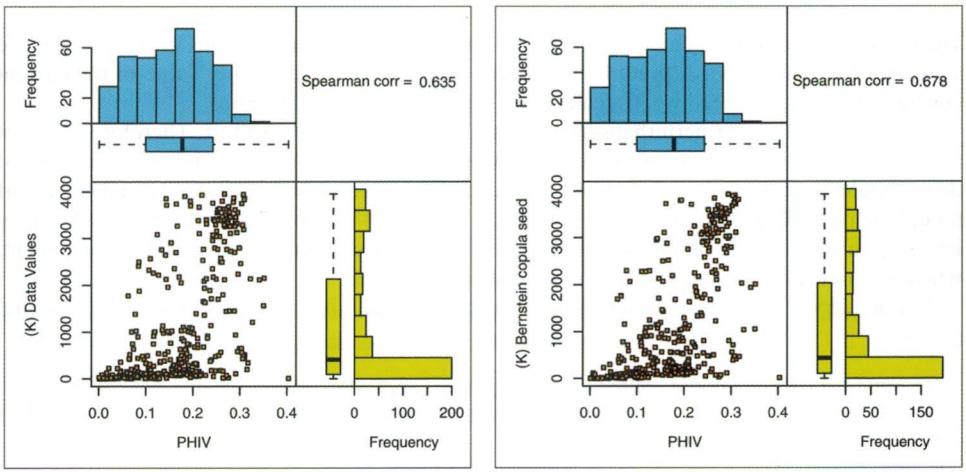

Figure 11.3 On the left, scatterplot of the original data, PHIV vs. K. On the right, the scatter plot of one single non-conditional simulation of PHIV vs. K, using Bernstein copulas, each scatter plot has their respective histograms.

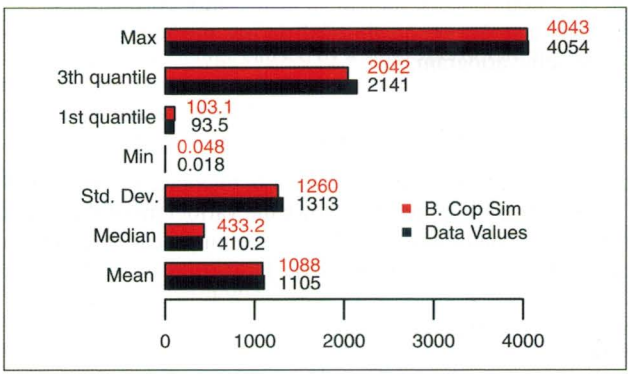

Figure 11.4 Comparative table and graph, of some statistics to real and simulated K values using Bernstein copulas.

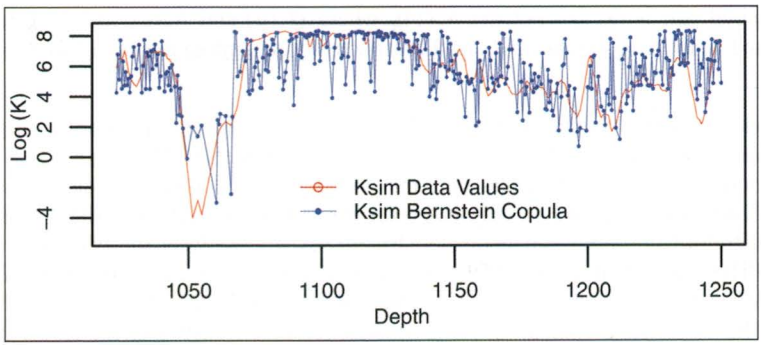

Figure 11.5 Spatial distribution of the real permeability and a simple non-conditional Bernstein copulas K simulation, using PHIV as secondary variable.

11.3.3 *Defining the objective function*

The simulated annealing technique runs many, often millions of perturbations in order to achieve an acceptable realization. A perturbation means modifying a permeability value of the current configuration, e.g. the seed we just calculated when the method just begins.

Executing millions of perturbations implies a high computational effort. Therefore, it is not recommended having too many components into the objective function, and also each one of them should be reasonably simple to compute, see Deutsch & Journel (1998). The advantage of model the dependence structure of petrophysical properties using Bernstein copulas is that they let us establish a simple objective function, i.e. an objective function with a single component, which does not affect the global computational performance.

The objective function is defined using the variogram, as it is proposed by Deutsch & Journel (1998).

$$FO = \sum_i \frac{[\gamma^*(h_i) - \gamma(h_i)]^2}{\gamma(h_i)^2} \tag{11.7}$$

where:

$$\gamma(h) = \frac{1}{2N(h)} \sum_{i=1}^{N(h)} [Z(x_i + h) - Z(x_i)]^2 \tag{11.8}$$

Deutsch and Cockerham methodology specifies the dependence structure through a multi-objective function, i.e. 5 components: individual histograms, correlation coefficient, variogram, indicator variogram and distribution conditional. In our methodology we propose the use of a single component, the semivariogram.

11.3.4 *Measuring the energy of the seed, according to the objective function*

It has been proposed a variogram in the direction of 0, tolerance of 90 (isotropic variogram), 50 intervals and a 2.27 meters lag. Figure 11.6 shows the variogram of the original data (objective function). Under the same conditions we calculate the empirical variogram and the model for seed configuration, see Figure 11.6. RGEOESTAD, Díaz-Viera et al. (2010), was used to analyze these results.

Using Equation (11.7) we obtain the initial energy:

$$E_i = 159.6313$$

In Table 11.1 they are shown the models to each configuration.

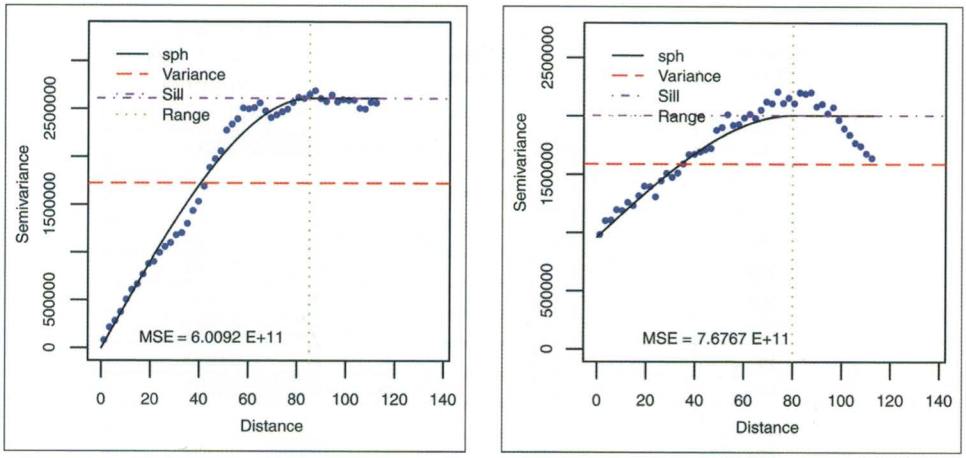

Figure 11.6 To the left, estimated variogram, 50 lag's for the data set. To the right, estimated variogram, 50 lag's for the seed.

Table 11.1 Variograms models to the dataset and seed.

	Nugget	Sill + Nugget	Range
Dataset	0.00	2611621.52	85.07
Seed	962645.81	2004671.28	80.00

11.3.5 *Calculating the initial temperature, and the most suitable annealing schedule of simulated annealing method to carry out the simulation*

To calculate the annealing schedule it is followed the procedure recommended by Dreo et al. (2006). The initial temperature is calculated based on Equation (11.9).

$$T_0 = \left(-\frac{\Delta E}{\log(\tau_0)}\right) \tag{11.9}$$

where ΔE ($E_{perturb} - E_{initial}$) is the mean of the energy differences between 100 perturbed configurations and the seed. The perturbation mechanism consists of uniformly and randomly chooses a value of porosity and generates a new permeability value using the simulation Bernstein copulas algorithm.

Each perturbation always starts in the same initial configuration. This is because our objective is to measure the system's energy change caused by a single perturbation. With this, we can get an idea of the acceptance rate (τ_0) we need to introduce. Let us remember that the rate of acceptance (τ_0) is a value that discriminates, within Boltzmann equation, the quality of a configuration that we will accept W. L. Coffee (1993). Therefore, an acceptance rate (τ_0) close to one will accept all perturbed configuration (low quality acceptance rate), while rates close to zero, only will accept perturbed configurations that reduce the overall system energy (high quality acceptance rate).

On Figure 11.7 they are shown 23 of the 100 perturbations of the initial configuration with an acceptance rate of 0.5 (medium quality). Also, it is made the calculation of each term of Equation (11.9) to show how metropolis criterion works to accept or reject the effect of a perturbation in the overall system energy.

Note that in the second column of this table that ΔE can have positive or negative differences, for example, 9.58 is a positive difference and corresponds to the energy of 169.21 (fifth row); or −2.69, which is a negative difference and corresponds to an energy of 156.93 (penultimate row). Positive differences indicate that the energy of the perturbed configuration is greater than the

100 perturbation energy vs. OF	ΔE	Metropolis acceptance (1)	- ΔE/T	Metropolis acceptance (2) Boltzmann $r < \exp(-\langle \Delta E \rangle / T)$
160.2733	0.6420	✗	-0.4835	0.6166
159.6089	-0.0224	✓		
159.6204	-0.0109	✓		
163.5322	3.9009	✗	-2.9381	0.0530
169.2158	9.5845	✗	-7.2189	0.0007
164.3231	4.6918	✗	-3.5338	0.0292
159.6924	0.0611	✗	-0.0460	0.9550
165.3448	5.7135	✗	-4.3033	0.0135
160.1211	0.4898	✗	-0.3689	0.6915
159.2698	-0.3615	✓		
161.3739	1.7426	✗	-1.3125	0.2691
159.6402	0.0089	✗	-0.0067	0.9933
159.6389	0.0076	✗	-0.0057	0.9943
159.5629	-0.0684	✓		
159.6319	0.0006	✗	-0.0005	0.9995
159.647	0.0157	✗	-0.0118	0.9882
160.4136	0.7823	✗	-0.5892	0.5548
162.3441	2.7128	✗	-2.0432	0.1296
159.6323	0.0010	✗	-0.0008	0.9992
159.9063	0.2750	✗	-0.2071	0.8129
156.9334	-2.6979	✓		
159.4875	-0.1438	✓		
159.3414	-0.2899	✓		

Figure 11.7 23 perturbations of the initial configuration with an acceptance rate of 0.5, plus the calculation of each term of Equation (11.9).

energy of the initial configuration, negative differences indicate that the energy of the perturbed configuration is less than the energy of the initial configuration. Therefore, using the Metropolis criterion in its first phase means that only the negative energy differences will be accepted (green check mark, third column of Figure 11.7 and positive differences will be rejected (red check mark).

In its second phase the metropolis criterion tries to accept certain configurations which initially were rejected. In last column of Figure 11.7 are calculated, using the expression $\exp(\Delta E/T)$, the probability of acceptance for each initially rejected energy. Based on what is shown in Figure 11.7, those perturbed configurations, that have a great positive energetic difference will have little chance of being accepted, while those perturbed configurations that have a small positive energetic difference will have a high probability to be accepted.

In Figure 11.8, they are shown the same 23 perturbations of the initial configuration, with a rate of acceptance of 0.01. Note that the smaller rate to acceptance, the lower probability of acceptance.

In Figure 11.9 they are shown the same 23 perturbations of the initial configuration, now with an acceptance rate of 0.99. Note that most of the perturbations initially rejected have a high probability of being accepted.

Finally, we consider an acceptance rate of 0.5, because the Bernstein copula generates a "good quality" seed. Therefore, using Equation (11.9) the initial temperature is:

$$T_0 = 1.14$$

100 perturbation energy vs. OF	ΔE	Metropolis acceptance (1)	- ΔE/T	Metropolis acceptance (2) Boltzmann $r < \exp(-\langle \Delta E \rangle / T)$
160.2733	0.6420	✗	-3.7248	0.0241
159.6089	-0.0224	✓		
159.6204	-0.0109	✓		
163.5322	3.9009	✗	-22.6324	0.0000
169.2158	9.5845	✗	-55.6077	0.0000
164.3231	4.6918	✗	-27.2210	0.0000
159.6924	0.0611	✗	-0.3545	0.7015
165.3448	5.7135	✗	-33.1488	0.0000
160.1211	0.4898	✗	-2.8417	0.0583
159.2698	-0.3615	✓		
161.3739	1.7426	✗	-10.1103	0.0000
159.6402	0.0089	✗	-0.0516	0.9497
159.6389	0.0076	✗	-0.0441	0.9569
159.5629	-0.0684	✓		
159.6319	0.0006	✗	-0.0035	0.9965
159.647	0.0157	✗	-0.0911	0.9129
160.4136	0.7823	✗	-4.5388	0.0107
162.3441	2.7128	✗	-15.7392	0.0000
159.6323	0.0010	✗	-0.0058	0.9942
159.9063	0.2750	✗	-1.5955	0.2028
156.9334	-2.6979	✓		
159.4875	-0.1438	✓		
159.3414	-0.2899	✓		

Figure 11.8 23 perturbations of the initial configuration with an acceptance rate of 0.01, plus the calculation of each term of Equation (11.9).

The change of stage is done by following the next conditions:

- $12 * N$ accepted perturbations $= 12 * 380 = 4500$
- $100 * N$ attempted perturbations $= 100 * 380 = 38000$

where N is the data number.

The decrease in temperature is calculated using geometric law Equation (11.10), see Figure 11.10.

$$T_{k+1} = 0.8 * T_k \tag{11.10}$$

11.3.6 *Performing the simulation*

The methodology proposed in this work is a simulation divided into two steps. First, we have to perturb the configuration system by generating a new permeability value, using bivariate Bernstein copulas simulation. Second, apply the simulated annealing method to generate a stochastic simulation accepting or rejecting the before perturbations, by using Metropolis criterion.

As it was mentioned in the previous section, each perturbation consists of generate a new permeability value (K), by the non-parametric and non-conditional simulation algorithm, using porosity (PHI) as a secondary variable. The Bernstein copulas suggest a new permeability value

100 perturbation energy vs. OF	ΔE	Metropolis acceptance (1)	- ΔE/T	Metropolis acceptance (2) Boltzmann $r < \exp\left(-\langle \Delta E \rangle / T\right)$
160.2733	0.6420	✗	-0.0081	0.9919
159.6089	-0.0224	✓		
159.6204	-0.0109	✓		
163.5322	3.9009	✗	-0.0494	0.9518
169.2158	9.5845	✗	-0.1214	0.8857
164.3231	4.6918	✗	-0.0594	0.9423
159.6924	0.0611	✗	-0.0008	0.9992
165.3448	5.7135	✗	-0.0723	0.9302
160.1211	0.4898	✗	-0.0062	0.9938
159.2698	-0.3615	✓		
161.3739	1.7426	✗	-0.0221	0.9782
159.6402	0.0089	✗	-0.0001	0.9999
159.6389	0.0076	✗	-0.0001	0.9999
159.5629	-0.0684	✓		
159.6319	0.0006	✗	0.0000	1.0000
159.647	0.0157	✗	-0.0002	0.9998
160.4136	0.7823	✗	-0.0099	0.9901
162.3441	2.7128	✗	-0.0343	0.9662
159.6323	0.0010	✗	0.0000	1.0000
159.9063	0.2750	✗	-0.0035	0.9965
156.9334	-2.6979	✓		
159.4875	-0.1438	✓		
159.3414	-0.2899	✓		

Figure 11.9 23 perturbations of the initial configuration with an acceptance rate of of 0.5, plus the calculation of each term of Equation (11.9).

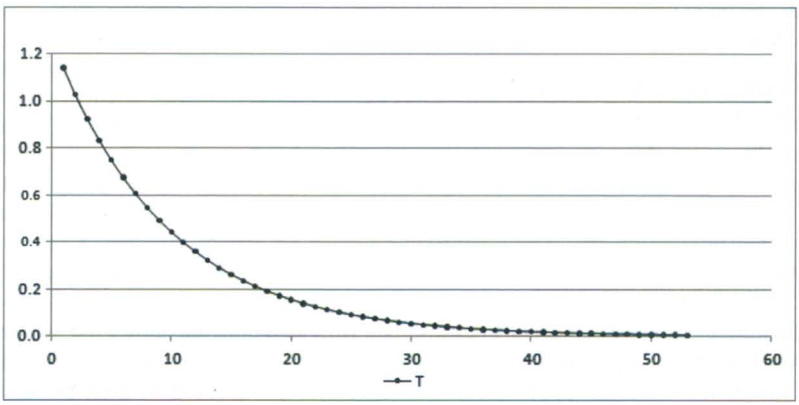

Figure 11.10 The geometric law is used to calculate the Decreasing program schedule of temperature, to perform the simulated annealing cooling.

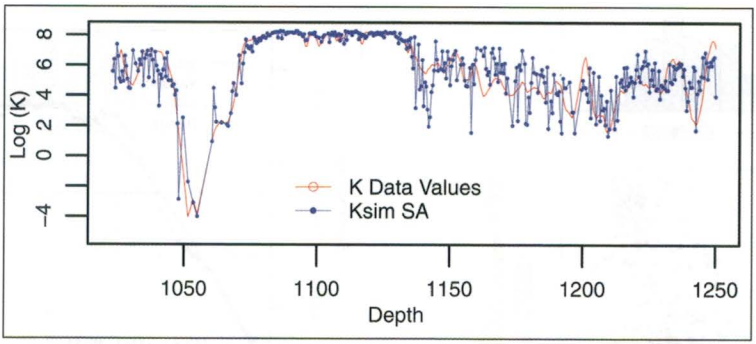

Figure 11.11 Spatial distribution of permeability in a single non-conditional SA simulation of K, with bivariate Bernstein copula, using PHIV as secondary variable.

which is well fitted within the dependence structure of these properties. This is what makes this approach attractive, because while traditional regression methods impose a linear dependence, Bernstein copulas allow modeling complex structures and nonlinear dependence that such methods do not. Therefore, each perturbation will always respect the relationship existing between the petrophysical properties.

The acceptance-rejection procedure also depends on the temperature of each stage when the simulation is in progress, so, it is necessary to allow the simulated annealing method to make a sufficient number of simulations for each temperature stage to reach its thermodynamic equilibrium. In other words, it is necessary to ensure that, by time of lowering the temperature, (phase change), the solution space has been sufficiently explored so that it contains the best solution.

Every time the temperature is decreased, the acceptance metropolis criterion becomes more restrictive, so that, at lower temperatures, only is accepted the best configurations, i.e. those with the lowest system energy.

The simulation finalizes when the objective function error is reached (previously defined); an accumulation of stages without change occurs; or when the maximum attempted perturbations is reached.

11.3.7 *Application of the methodology for stochastic simulation by bivariate Bernstein copulas to simulate a permeability (K) profile. A case of study*

We model the relationship between the permeability and porosity of the double porosity carbonate formations of a South Florida aquifer in the western Hillsboro Basin of Palm Beach County, Florida, see Figure 11.2. Until now, we have used bivariate Bernstein copulas to obtain an initial configuration (seed); also we have proposed an objective function and using it to measure the energy of the seed; finally we have calculated the initial temperature and the schedule program to perform the geostatistical simulation with simulated annealing. Figure 11.11, shows a single non-conditional and non-parametric simulated annealing simulation of K using PHIV (vuggy porosity) as a secondary variable. The simulation shows that the permeability values follow the spatially pattern as the original data, although, even now there is still small-scale variability on results, but it is smaller than the seed.

Figure 11.12 shows the scatterplot between K and PHIV from single non-conditional SA simulation using bivariated Bernstein copula and their respective histograms. As we could anticipate, the dependence structure between this two petrophysical properties is well represented. In the same Figure 11.12, it is shown the empirical variogram and its model (objective function) of the simulation.

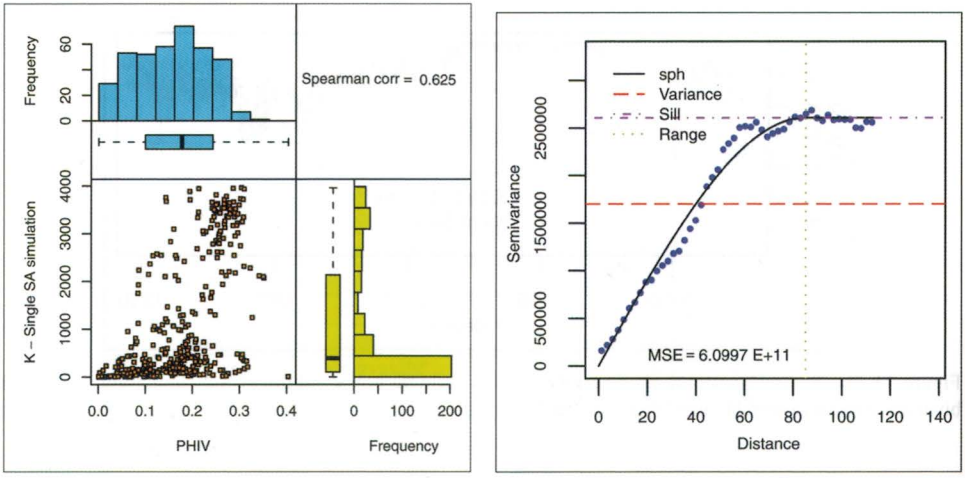

Figure 11.12 Scatter plot and variogram of a single non-conditional simulated annealing simulation for K using PHIV as a secondary variable.

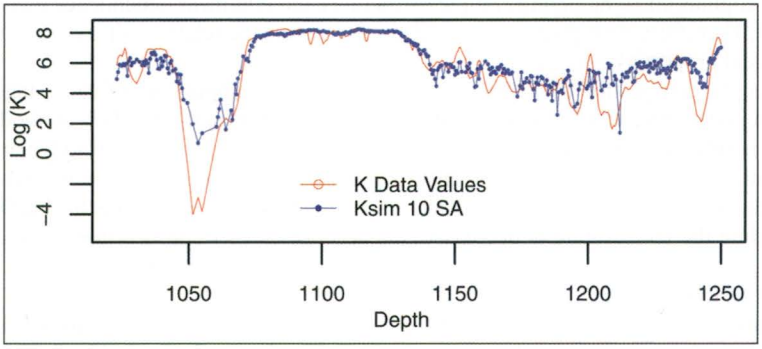

Figure 11.13 Spatial distribution of permeability in a median of 10 non-conditional SA simulations of K, with bivariate Bernstein copula, using PHIV as secondary variable.

Also it was realized a median of 10 non-conditional simulated annealing simulations in order to reduce small-scale variability, see Figure 11.13.

We put also the median scatter plot and its respective variogram, Figure 11.14. The reason for using a median rather than an average is because the median is not skewed as easily as the average.

As it can be seen in the median of 10 simulations, it is also very well represented the bivariate dependence structure of porosity-permeability relationship. Below is presented a comparative table of the variogram models, see Table 11.2.

As it can be seen, in the 10 median simulations is also very well represented the bivariate dependence structure of porosity-permeability relationship.

All simulations (including seed) have very similar statistics, Figure 11.15, this is because the dependence structure of the petrophysical properties is been modeled by Bernstein copulas. In the same figure, the bar labeled as K SA 1, which represents a simple simulation, is the best approaching to the original data, the bar labeled as Data; followed by the median of the 10 simulations, the bar labeled as K SA Median, this is because although the median smooths the variability of each simulation also accumulates each one of their mistakes; finally the seed, the bar labeled as K Seed.

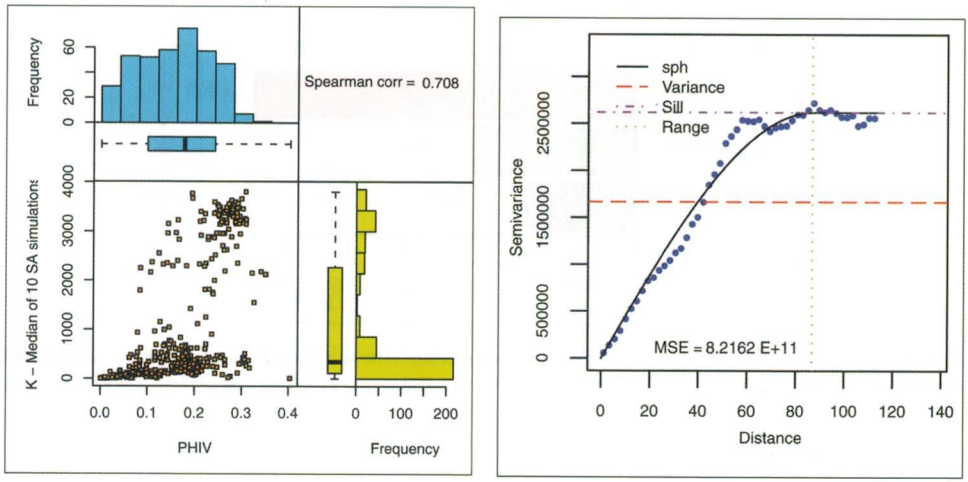

Figure 11.14 Scatter plot and variogram of a median of 10 non-conditional SA simulations of K using PHIV as a secondary variable.

Table 11.2 Variograms Models of the Dataset, seed, single non-conditional SA simulation and the median of 10 SA non-conditional simulations.

Configuration	Nugget	Sill + Nugget	Range
Dataset	0.00	2.61162×10^6	85.07
Seed	962645.81	2.00467×10^6	80.00
K SA 1	0.00	2.612×10^6	84.99
K SA Median	0.00	2.620×10^6	86.84

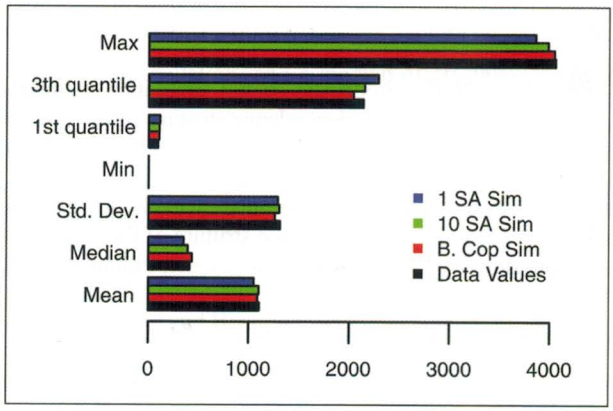

Figure 11.15 Statistical comparison of to the original data, initial configuration, a single SA simulation, and the median of 10 SA simulations.

Finally, Figure 11.16 shows a comparison chart of the mean square error (MSE). As we can see the values that have the greatest MSE are the data of the seed, 3.309. The simulated annealing simulations using bivariate Bernstein copulas, single and median shows MSE very reduced 1.415 and 0.921 respectively.

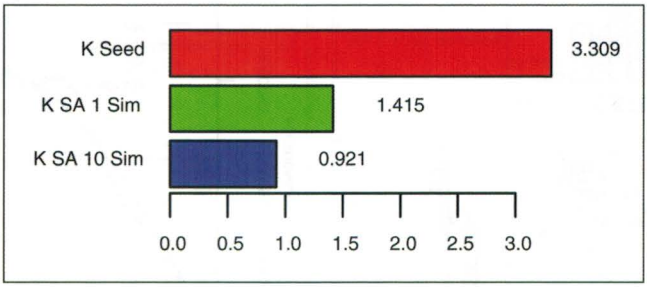

Figure 11.16 Mean Square Error (MSE) comparison between the initial configuration (seed), a single SA simulation, and the median of 10 SA simulations.

11.4 COMPARISON OF RESULTS USING THREE DIFFERENT METHODS

We propose the use of Bernstein copulas instead of establishing linear function using semi-logarithmic transformations, because they eventually end up giving results that are far away from the real data distribution. Also we say that a parametric copula based approach can represent very well a simple distribution structure but in data with complex relationship, the data may not to be naturally estimated, due the real data distribution is hard to fit properly with only one kind of distribution.

In this section we perform a comparative analysis between three methodologies used to simulate the spatial distribution of permeability (K), using its dependence structure with the petrophysical property: vuggy porosity (PHIV). The purpose of this analysis is to demonstrate that the Bernstein copulas is a better and sophisticated tool.

The comparison of permeability simulations is performed using the following methodologies:

1. Sasim of GSLIB Deutsch & Jouenel (1998). Stochastic simulation methodology by simulated annealing whose multiobjective function consists of two individual histograms, a correlation coefficient, a semivariogram moldel, and its conditional distribution, Equations (11.11, 11.12, 11.4 & 11.15).
2. *t*-copula Díaz-Viera et al. (2005). Stochastic spatial simulation methodology by simulated annealing using *t*-copulas to model the dependence struture of the petrophysical properties. Its multiobjective function is composed of the correlation coefficient, a semivariogram model, and conditional distribution, Equations (11.12, 11.14 & 11.15).
3. Bivariate Bernstein copulas. Stochastic spatial simulation methodology by simulated annealing using Bernstein copulas to model the dependence struture of the petrophysical properties. Its objective function consists only of a semivariogram model, Equation (11.12).

Here are the equations to calculate the objective function:

$$O_1 = \sum_z [F^*(z) - F(z)]^2 \tag{11.11}$$

$$O_2 = \sum_h \left[\frac{\gamma^*(h) - \gamma(h)]^2}{\gamma(h)^2} \right] \tag{11.12}$$

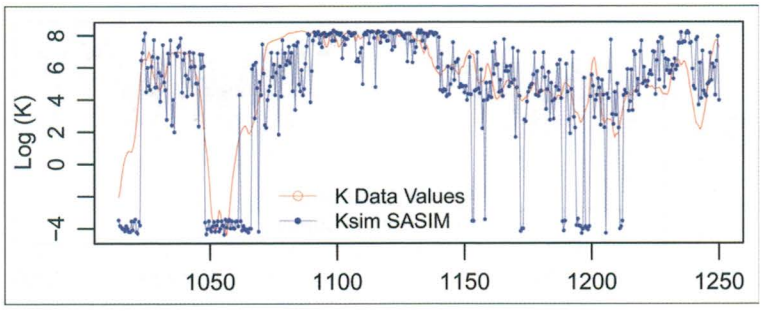

Figure 11.17 Spatial distribution in a single non-conditional simulation using SASIM methodology (Deutsch 1998), and using PHIV as a secondary variable.

where:

$$\gamma(h) = \frac{1}{2N(h)} \sum_{i=1}^{N(h)} [Z(x_i + h) - Z(x_i)]^2 \tag{11.13}$$

$$O_3 = [\rho^* - \rho]^2 \tag{11.14}$$

$$O_4 = \sum_{j=0}^{n_s} \sum_{i=0}^{n_p} [f_i^*(j) - f_i(j)]^2 \tag{11.15}$$

Before beginning, an overview of the performed comparisons using the three methodologies is presented:

- A single non-conditional simulation, and a median of 10 non-conditional simulations of permeability profile.
- A single 10% conditional simulation, and a median of 10, 10% conditional simulations of permeability profile.
- A single 50% conditional simulation, and a median of 10, 50% conditional simulations of permeability.
- A single 90% conditional simulation, and a median of 10, 90% conditional simulations of permeability profile.

11.4.1 *A single non-conditional simulation, and a median of 10 non-conditional simulations of permeability*

Figures 11.17, 11.18 & 11.19 show the spatial distribution of permeability in a single non-conditional simulation with simulated annealing, using as secondary variable PHIV. Simulation methodologies: SASIM. *t*-copula and Bivariate Bernstein copula.

A complete table of the MSE's differences between each method, in terms of percentage, is presented below (Table 1.3). Note that the methodology with the greater mean square error is SASIM with a value of 7.76, it is followed by the *t*-copula with 5.55 (which represents the 71% respecting SASIM-GSLib methodology) after the Bernstein copulas appear with a value of 1.85 (which represents the 23% respecting SASIM-GSLib methodology).

Figures 11.20, 11.21 & 11.22 show the comparison of the spatial distribution of the permeability of a median of 10 non-conditional simulations with simulated annealing, using PHIV as a secondary variable. Simulation methodologies: SASIM. *t*-copula and Bivariate Bernstein copula.

A complete table of the MSE's differences between each method, in terms of percentage, is presented (Table 11.4). Once again the methodology with a greater mean square error is the

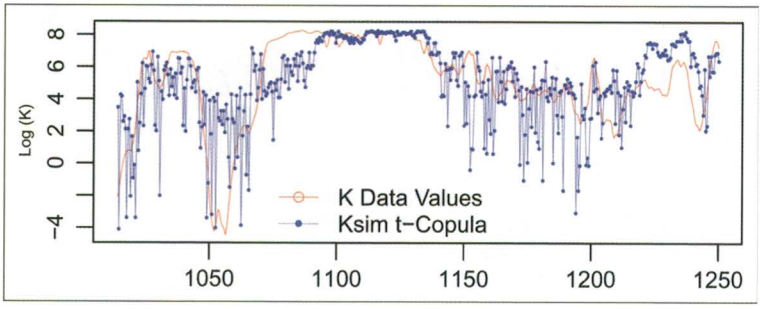

Figure 11.18 Spatial distribution in a single non-conditional simulation using *t*-copula methodology (Díaz et al. 2005), and using PHIV as a secondary variable.

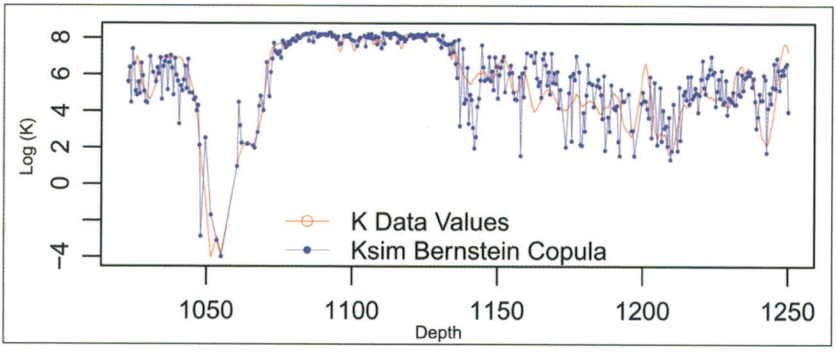

Figure 11.19 Spatial distribution in a single non-conditional simulation using Bivariate Bernstein copula methodology, and using PHIV as a secondary variable.

Table 11.3 Complete table of error differences between each method in terms of percentage. For a single simulation.

Method	MSE	vs. SASIM	vs. *t*-Copula
SASIM	7.76	100%	–
t-Copula	5.55	71.5%	100%
Bernstein Copula	1.85	23.8 %	33.3%

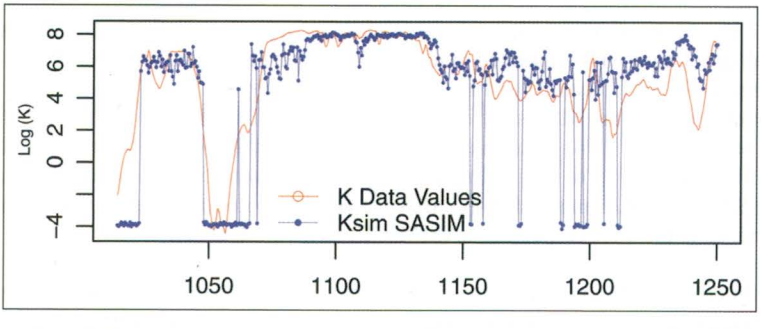

Figure 11.20 Spatial distribution in a median of 10 non-conditional simulations using SASIM methodology (Deutsch 1998), and using PHIV as a secondary variable.

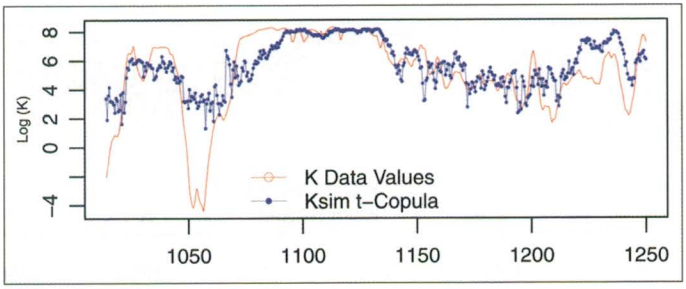

Figure 11.21 Spatial distribution in a median of 10 non-conditional simulations using *t*-copula methodology (Díaz et al. 2005), and using PHIV as a secondary variable.

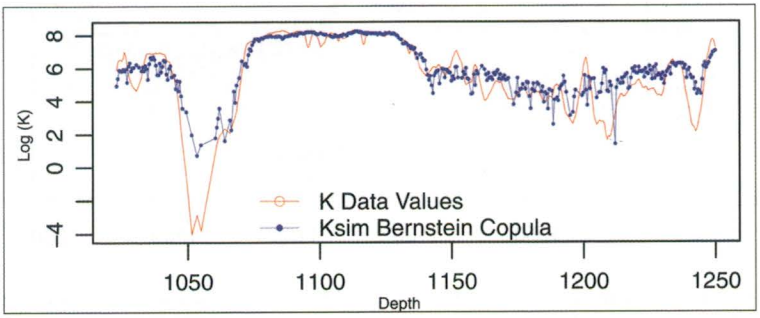

Figure 11.22 Spatial distribution in a median of 10 non-conditional simulations using Bivariate Bernstein copula methodology, and using PHIV as a secondary variable.

Table 11.4 Complete table of error differences between each method in terms of percentage. For a median of 10 nonconditional simulations.

Method	MSE	vs. SASIM	vs. *t*-Copula
SASIM	7.00	100%	–
t-Copula	3.82	54.6%	100%
Bernstein Copula	1.17	16.7%	30.6%

performed with SASIM with a value of 7.00 followed by the *t*-copula with 3.82 (which represents the 54% respecting SASIM-GSLib methodology) after copulas Bernstein appear with a value of 1.17 (which represents the 16% respecting SASIM-GSLib methodology).

Between 1 and 10 simulations, each methodology has a MSE reduction, 9% for SASIM (from 7.76 to 7.00); 31% for the t-copulas (from 5.55 to 3.82); 36% for Bernstein copulas (from 1.85 to 1.17).

11.4.2 *A single 10% conditional simulation, and a median of 10, 10% conditional simulations of permeability*

The Figure 11.23, 11.24 & 11.25 show the spatial distribution of permeability in a single 10% conditional simulation using as secondary variable PHIV. Simulation methodologies: SASIM. *t*-copula and Bivariate Bernstein copula.

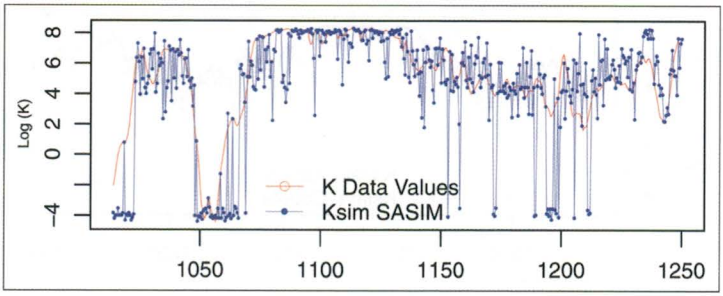

Figure 11.23 Spatial distribution in a single 10% conditional simulation using SASIM methodology (Deutsch 1998), and using PHIV as a secondary variable.

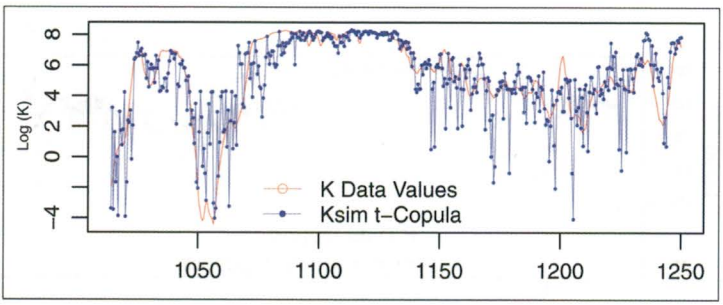

Figure 11.24 Spatial distribution in a single 10% simulation using *t*-copula methodology (Díaz et al. 2005), and using PHIV as a secondary variable.

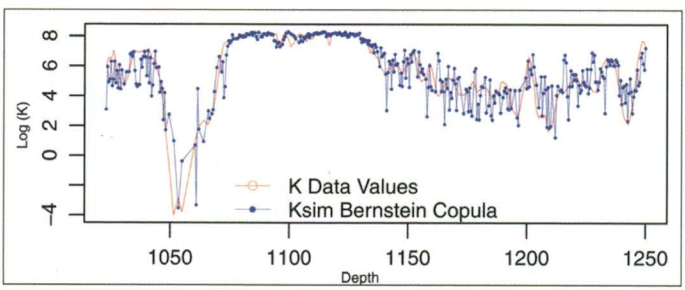

Figure 11.25 Spatial distribution in a single 10% simulation using Bivariate Bernstein copula methodology, and using PHIV as a secondary variable.

A complete table of the MSE's differences between each method, in terms of percentage, is presented (Table 1.5). Note that the methodology with a greater mean square error is the performed with SASIM with a value of 6.66 followed by the *t*-copula with 3.58 (which represents the 54% respecting SASIM-GSLib methodology) after copulas Bernstein appear with a value of 1.42 (which represents the 21% respecting SASIM-GSLib methodology).

Figures 11.26, 11.27 and 11.28 show the comparison of the spatial distribution of the permeability of a median of 10, 10% conditional simulations with simulated annealing, using PHIV as a secondary variable. Simulation methodologies: SASIM. *t*-copula and Bivariated Bernstein copula.

A complete table of the MSE's differences between each method, in terms of percentage, is presented (Table 1.6). Once again the methodology with a greater mean square error is the performed with SASIM with a value of 5.91 followed by the *t*-copula with 2.90 (which represents

Table 11.5 Complete table of error differences between each method in terms of percentage. For a single 10% conditional simulation.

Method	MSE	vs. SASIM	vs. *t*-Copula
SASIM	6.66	100%	–
t-Copula	3.58	53.8%	100%
Bernstein copula	1.42	21.3%	39.7%

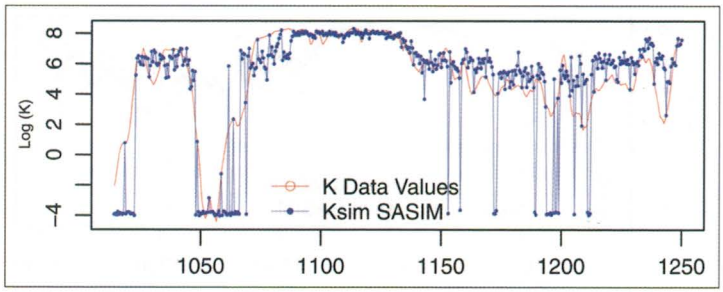

Figure 11.26 Spatial distribution in a median of 10, 10% conditional simulations using SASIM methodology (Deutsch 1998), and using PHIV as a secondary variable.

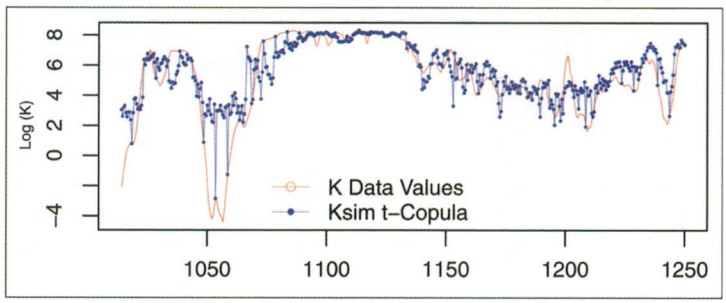

Figure 11.27 Spatial distribution in a median of 10, 10% conditional simulations using *t*-copula methodology (Díaz et al. 2005), and using PHIV as a secondary variable.

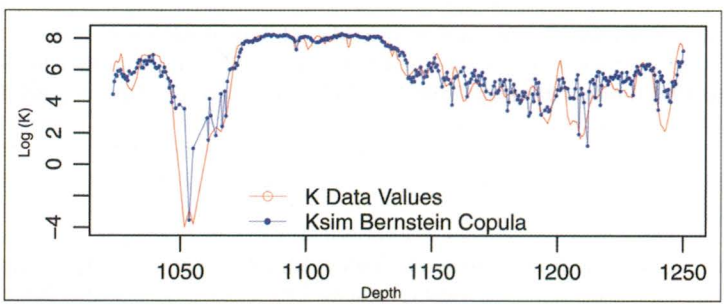

Figure 11.28 Spatial distribution in a median of 10, 10% conditional simulations using bivariate Bernstein copula methodology, and using PHIV as a secondary variable.

Table 11.6 Complete table of error differences between each method in terms of percentage. For a median of 10% conditional simulations.

Method	MSE	vs. SASIM	vs. *t*-Copula
SASIM	5.91	100%	–
t-Copula	2.90	49.1%	100%
Bernstein copula	1.02	17.3%	35.2%

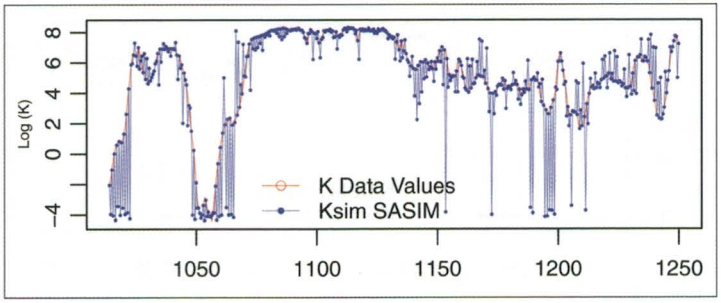

Figure 11.29 Spatial distribution in a single 10% conditional simulation using SASIM methodology (Deutsch 1998), and using PHIV as a secondary variable.

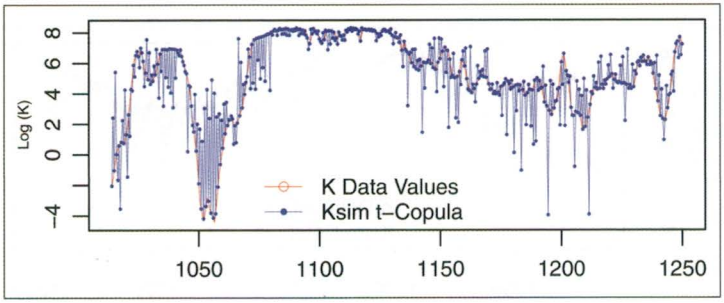

Figure 11.30 Spatial distribution in a single 10% simulation using *t*-copula methodology (Díaz et al. 2005), and using PHIV as a secondary variable.

the 49% respecting SASIM-GSLib methodology) after copulas Bernstein appear with a value of 1.02 (which represents the 17% respecting SASIM-GSLib methodology).

Between 1 and 10 simulation, each methodology has a MSE reduction, 11% for SASIM (from 6.66 to 5.91); 19% for the t-copulas (from 3.82 to 2.90); 36% for Bernstein copulas (from 1.42 to 1.02).

11.4.3 *A single 50% conditional simulation, and a median of 10, 50% conditional simulations of permeability*

The Figure 11.29, 11.30 and 11.31 show the spatial distribution of permeability in a single 50% conditional simulation using as secondary variable PHIV. Simulation methodologies: SASIM. *t*-copula and Bivariate Bernstein copula.

A complete table of the MSE's differences between each method, in terms of percentage, is presented below (Table 1.7). Note that the methodology with a greater mean square error is the

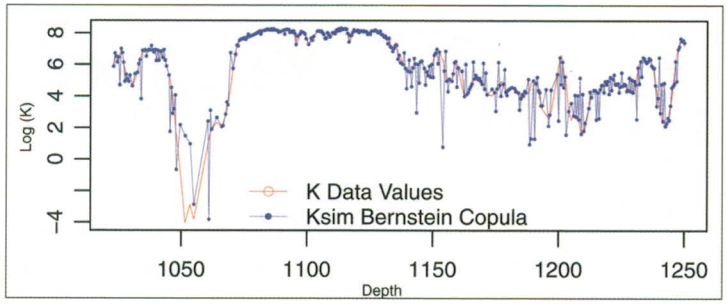

Figure 11.31 Spatial distribution in a single 10% simulation using Bivariate Bernstein copula methodology, and using PHIV as a secondary variable.

Table 11.7 Complete table of error differences between each method in terms of percentage. For a single 50% conditional simulation.

Method	MSE	vs. SASIM	vs. *t*-Copula
SASIM	3.22	100%	–
t-Copula	2.56	79.5%	100%
Bernstein copula	0.88	34.4%	34.4%

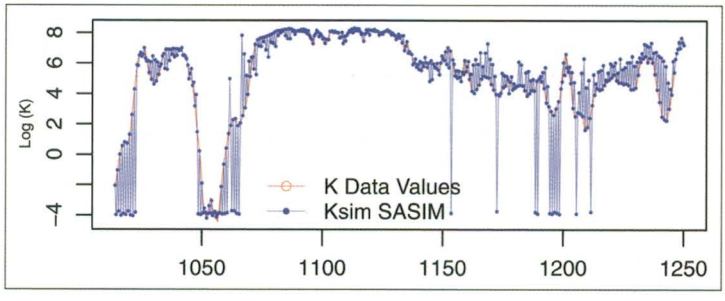

Figure 11.32 Spatial distribution in a median of 10, 50% conditional simulations using SASIM methodology (Deutsch 1998), and using PHIV as a secondary variable.

performed with SASIM with a value of 3.22 followed by the *t*-copula with 2.56 (which represents the 51% respecting SASIM-GSLib methodology) after Bernstein copulas appear with a value of 0.88 (which represents the 21% respecting SASIM-GSLib methodology).

Figures 11.32, 11.33 & 11.34 show the comparison of the spatial distribution of the permeability of a median of 10 50% conditional simulations with simulated annealing, using PHIV as a secondary variable. Simulation methodologies: SASIM. *t*-copula and Bivariated Bernstein copula.

A complete table of the MSE's differences between each method, in terms of percentage, is presented below (Table 1.8). Once again the methodology with a greater mean square error is the performed with SASIM with a value of 3.04 followed by the *t*-copula with 1.65 (which represents the 54% respecting SASIM-GSLib methodology) after Bernstein copulas appear with a value of 0.53 (which represents the 17% respecting SASIM-GSLib methodology).

Between 1 and 10 simulation, each methodology has a MSE reduction, 8% for SASIM (from 3.22 to 3.04); 35% for the t-copulas (from 2.56 to 1.65); 39% for Bernstein copulas (from 0.88 to 0.53).

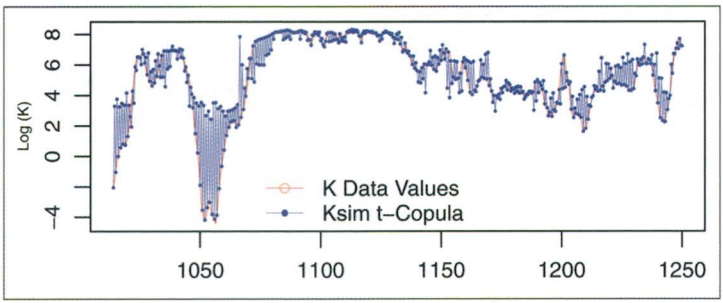

Figure 11.33 Spatial distribution in a median of 10, 50% conditional simulations using *t*-copula methodology (Díaz et al. 2005), and using PHIV as a secondary variable.

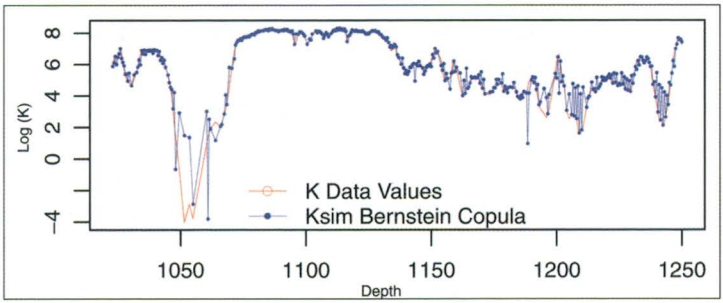

Figure 11.34 Spatial distribution in a median of 10, 50% conditional simulations using Bivariate Bernstein copula methodology, and using PHIV as a secondary variable.

Table 11.8 Complete table of error differences between each method in terms of percentage. For a median of 50% conditional simulations.

Method	MSE	vs. SASIM	vs. *t*-Copula
SASIM	3.04	100%	–
t-Copula	1.65	54.3%	100%
Bernstein copula	0.53	17.4%	32.1%

11.4.4 *A single 90% conditional simulation, and a median of 10, 90% conditional simulations of permeability*

The Figure 11.35, 11.36 & 11.37 show the spatial distribution of permeability in a single 90% conditional simulation using as secondary variable PHIV. Simulation methodologies: SASIM. *t*-copula and Bivariate Bernstein copula.

A complete table of the MSE's differences between each method, in terms of percentage, is presented below (Table 1.9). Note that the methodology with a greater mean square error is the performed with SASIM with a value of 0.92 followed by the *t*-copula with 0.51 (which represents the 44% respecting SASIM-GSLib methodology) after Bernstein copulas appear with a value of 0.40 (which represents the 55% respecting SASIM-GSLib methodology).

Figures 11.38, 11.39 and 11.40 show the comparison of the spatial distribution of the permeability of a median of 10 50% conditional simulations with simulated annealing, using PHIV as a secondary variable. Simulation methodologies: SASIM. *t*-copula and Bivariate Bernstein copula.

A complete table of the MSE's differences between each method, in terms of percentage, is presented below (Table 1.10). Once again the methodology with a greater mean square error is the

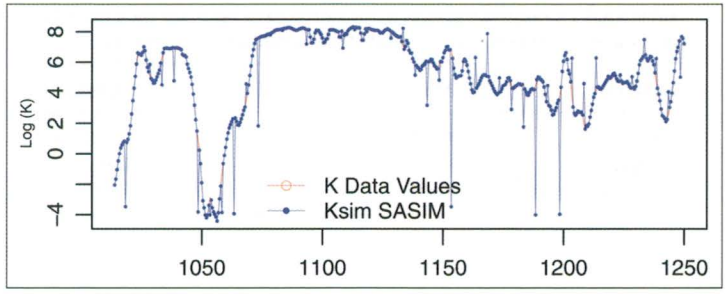

Figure 11.35 Spatial distribution in a single 90% conditional simulation using SASIM methodology (Deutsch 1998), and using PHIV as a secondary variable.

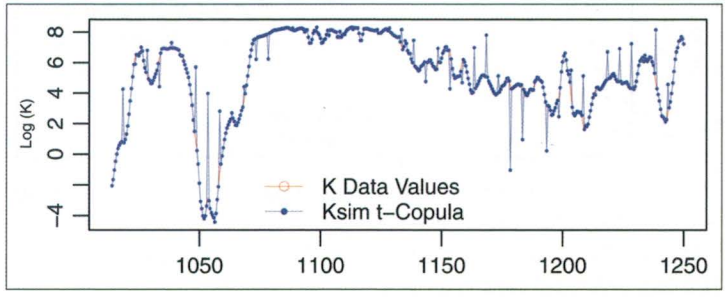

Figure 11.36 Spatial distribution in a single 90% simulation using *t*-copula methodology (Díaz-Viera et al. 2005), and using PHIV as a secondary variable.

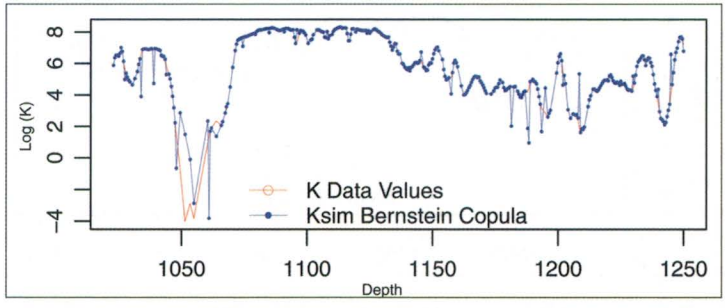

Figure 11.37 Spatial distribution in a single 90% simulation using Bivariate Bernstein copula methodology, and using PHIV as a secondary variable.

performed with SASIM with a value of 0.81 followed by the *t*-copula with 0.40 (which represents the 51% respecting SASIM-GSLib methodology) after copulas Bernstein appear with a value of 0.33 (which represents the 59% respecting SASIM-GSLib methodology).

Between 1 and 10 simulation, each methodology has a MSE reduction, 12% for SASIM (from 0.92 to 0.81); 21% for the t-copulas (from 0.51 to 0.40); 17% for Bernstein copulas (from 0.40 to 0.33).

11.5 CONCLUSIONS

The proposed method provides a very flexible tool to model the complex dependence relationships between pairs of petrophysical properties such as porosity and permeability. It can model bivariate

Table 11.9 Complete table of error differences between each method in terms of percentage. For a single 90% conditional simulation.

Method	MSE	vs. SASIM	vs. *t*-Copula
SASIM	0.92	100%	–
t-Copula	0.51	55.4%	100%
Bernstein copula	0.40	43.5%	78.4%

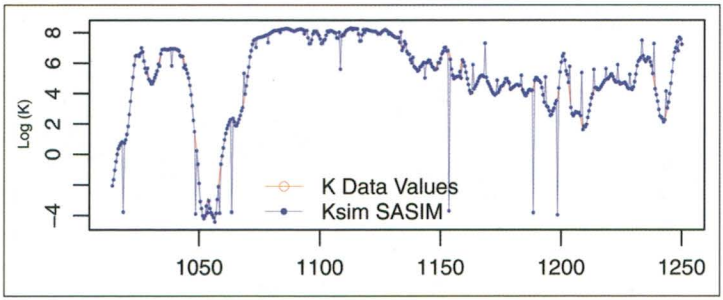

Figure 11.38 Spatial distribution in a median of 10, 90% conditional simulations using SASIM methodology (Deutsch 1998), and using PHIV as a secondary variable.

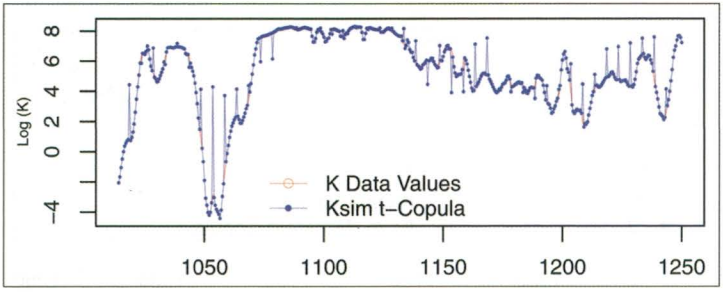

Figure 11.39 Spatial distribution in a median of 10, 90% conditional simulations using *t*-copula methodology (Díaz-Viera et al. 2005), and using PHIV as a secondary variable.

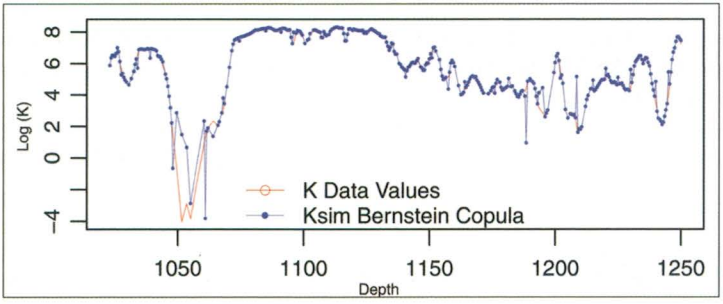

Figure 11.40 Spatial distribution in a median of 10, 90% conditional simulations using bivariate Bernstein copula methodology, and using PHIV as a secondary variable.

Table 11.10 Complete table of error differences between each method in terms of percentage. For a median of 90% conditional simulations.

Method	MSE	vs. SASIM	vs. *t*-Copula
SASIM	0.81	100%	–
t-Copula	0.40	49.4%	100%
Bernstein copula	0.33	40.7%	82.5%

dependencies in a much more efficient and accurate way. Hence, it serves as an alternative to traditional methods like linear regression, since it does not need the assumption of the existence of a linear dependency model between variables.

The methodology used in this work has three main advantages: First, an easy way to simulate bivariate data with the dependence structure and marginal behavior suggested by already observed data; second, a straightforward way to perform nonparametric quantile regression; and third, an easy way to implement a nonparametric copula into a stochastic geostatistical simulation.

In contrast to the parametric approach, the nonparametric one allows us to model non linear relationship between petrophysical properties without assume any distribution function as *t*-copula does, because the Bernstein copula is based on the empirical distribution function, and consequently, the may reproduce the data variability and the extreme values in a more natural way.

Since all the information about the dependence structure is contained in the underlying copula, in simulated annealing results, the histogram of permeability and porosity are automatically reproduced. Hence, the objective function is reduced and consequently its computational cost is lowered, we can take this advantage to introduce other components to objective function in order to get a better solution.

Another advantage about using the Bernstein copula is that there is no need to make logarithmic transformations of permeability, i.e. we do not have to make back transformations that can potentially bias the results. In fact, copulas are invariant under strictly increasing transformations of the variables.

In the case study, in contrast with the other two methods, SASIM of GSLIB and *t*-copula, the Bernstein copula has a mean squared error reduction about 83% (from 7.00 to 1.17) in non conditional simulations, consequently, it has more accurate results. It is necessary to say that there must be implemented efficient computational algorithms in order to speed up the computing time, because the Bernstein copula increases the computational effort in higher dimensions.

In this study case we noted that if we just performed a nonparametric quantile regression we obtain results that can compete (spatially speaking) with simulated annealing results (1.83 Bernstein copula median regression vs. 1.85 a single SA simulation).

The use of nonparametric copulas opens a promising line of research to model complex dependence structures between petrophysical properties and their intrinsic spatial dependence. In the geostatistical simulation framework, to make joint simulations we propose to use simulated annealing method, but we can use another optimization method which may give us more accurate results.

REFERENCES

Balan, B., Mohaghegh, S. & Ameri, S. (1995) State-of-the-art in permeability determination from well log data: Part 1. A comparative study, model development. *SPE 30978.*

Bennett, W.M., Linton, P.F. & Rectenwald, E.E. (2002) Hydrologic investigation of the Floridian aquifer system, western Hillsboro Basin, Palm Beach County, Florida. *Technical Publication WS-8.* South Florida Management District.

Billingsley, P. (1995) *Probability and Measure.* 3rd edition. New York, Wiley.

Deheuvels, P. (1979) La fonction de dépendance empirique et ses porpriétés. Un test nonparamétrique d'independance, *Académic Royale de belgique. Bulletin de la clane Sciences (5)*, 65(6): 274–292.

Deutsch, C.V. & Cockerham, P.W. (1994) Geostatistical modeling of permeability with annealing cosimulation (ACS). *SPE 28413.*

Deutsch, C.V. & Andre G. Journel. (1998) *GSLIB: Geostatistical Software Library and User's Guide*. 2nd edition. Oxford University Press, Oxford, U.K.: 369 pp.

Díaz-Viera, M., Barandela, A., Utset, R. & Fernandez, C. (1994) GEOESTAD: un sistema de computación para aplicaciones geoestadísticas. In: Barandela, R. (ed.). *Proceedings of GEOINFO*, 2nd Iberoamerican Workshop on Geomathematics, Havana.

Díaz-Viera, M. & Casar-González, R. (2005) Stochastic simulation of complex dependency patterns of petrophysical properties using t-copulas. *Proceedings IAMG'05: GIS and Spatial Analysis*, 2, 749–755.

Díaz-Viera, M., Anguiano-Rojas, P., Mousatov A., Kazatchenko E. & Markov M. (2006) Stochastic modeling of permeability in double porosity carbonates applying a Monte-Carlo simulation method with *t*-copulas. *SPWLA 47th Annual Logging Symposium*, Veracruz, Mexico, 4–7 June 2006.

Díaz-Viera, M., Hernández-Maldonado, V. & Mendez-Venegas, J. (2010) RGEOESTAD: Un programa de código abierto para aplicaciones geoestadísticas basado en R-Project, México. Available from: *http://mmc2.geofisica .unam.mx/gmee/paquetes.html.*

Dréo, J., Pétrowski, A., Siarry, P. & Taillard, T. (2006) *Metaheuristics for Hard Optimization*. Berlin, Heidelberg, Springer-Verlag.

Erdely, A. & Díaz-Viera, M.A. (2010) Nonparametric and semiparametric bivariate modeling of petrophysical porosity-permeability dependence from well log data. (Chapter 13). In. Jaworski, P., Durante, F., Hrdle, W.K. & Rychlik, T. (eds.). *Copula Theory and Its Applications*, *Lecture Notes in Statistics*, 198. Berlin Heidelberg, Springer-Verlag, pp. 267–278.

Fermanian, J-D. Radulović, D & Wegcamp M. (2004) Weak convergence of empirical copula processes. *Bernoulli*, 10, 847–860.

Kazatchenko, E., Markov, M. & Mousatov, A. (2004) Joint inversion of acoustic and resistivity data for carbonate microstructure evaluation. *Petrophysics*, 45, 130–140.

Kazatchenko, E., Markov, M., Mousatov, A. & Parra, J. (2006a) Carbonate microstructure determination by inversion of acoustic and electrical data: application to a South Florida Aquifer. *Journal of Applied Geophysics*, 59, 1–15.

Kazatchenko, E., Markov, M. & Mousatov, A. (2006b) Simulation of the acoustical velocities, electrical and thermal conductivities using unified pore structure model of double-porosity carbonate rocks. *Journal of Applied Geophysics*, 59, 16–35.

Muñoz-Pérez, J. & Fernández-Palacín, A. (1987) Estimating the quantile function by Bernstein polynomials. *Computational Statistics and Data Analysis*, 5, 391–397.

Nelsen, R. B. (2006) *An Introduction to Copulas*. 2nd edition. New York, Springer.

Parra, J.O., Hackert, C.L., Collier, H.A. & Bennett, M. (2001) A methodology to integrate magnetic resonance and acoustic measurements for reservoir characterization. *Report DOE/BC/ 15203-3*. Tulsa, Oklahoma, National Petroleum Technology Office, Department of Energy.

Parra, J.O. & Hackert, C.L. (2002) Permeability and porosity images based on crosswell reflection seismic measurements of a vuggy carbonate aquifer at the Hillsboro site, South Florida. *72nd Annual Meeting of the Society of Exploration Geophysicists*. Paper VCD P1.2.

Sancetta, A. (2007) Non-parametric estimation of distributions with given marginals via Bernstein–Kantorovic polynomials: L_1 and pointwise convergence theory. *Journal of Multivariate Analysis*, 98, 1376–1390.

Sancetta, A. & Satchell, S. (2004) The Bernstein copula and its applications to modeling and approximations of multivariate distributions. *Econometric Theory*, 20, 535–562.

Schweizer, B. & Sklar, A. (1983) *Probabilistic Metric Spaces*. New York, North Holland.

Sklar, A. (1959) Fonctions de répartition á *n* dimensions et leurs marges. *Publications de l'Institut de statistique de l'Université de Paris*, 8, 229–231.